



HAL
open science

Study of the Multifrequency Susceptibility of Operational Amplifiers

Alexandre Boyer, Fabrice Caignet

► **To cite this version:**

Alexandre Boyer, Fabrice Caignet. Study of the Multifrequency Susceptibility of Operational Amplifiers. EMC Europe 2024 Symposium, Sep 2024, Brugges, Belgium. <10.1109/EMCEurope59828.2024.10722498>. <hal-04689775>

HAL Id: hal-04689775

<https://laas.hal.science/hal-04689775v1>

Submitted on 6 Sep 2024

HAL is a multi-disciplinary open access archive for the deposit and dissemination of scientific research documents, whether they are published or not. The documents may come from teaching and research institutions in France or abroad, or from public or private research centers.

L'archive ouverte pluridisciplinaire HAL, est destinée au dépôt et à la diffusion de documents scientifiques de niveau recherche, publiés ou non, émanant des établissements d'enseignement et de recherche français ou étrangers, des laboratoires publics ou privés.



HAL Authorization

Study of the Multifrequency Susceptibility of Operational Amplifiers

A. Boyer^{#1}, F. Caignet^{#2}

[#]LAAS-CNRS, Univ. de Toulouse, INSA, UPS, LAAS, France

{¹alexandre.boyer, ²fcaignet}@laas.fr

Abstract — This paper deals with the susceptibility of operational amplifiers (op-amps) in multifrequency injection. After an in-depth analysis of the different failure mechanisms that induces DC-offset based on experimental results on a general-purpose op-amp, the paper proposes a risk assessment method based on continuous wave susceptibility test results.

Keywords —susceptibility, operational amplifier, multitone disturbance, integrated circuits.

I. INTRODUCTION

Immunity to electromagnetic (EM) disturbance is an essential requirement for electronic equipment to ensure a safe operation. It is strongly related to the susceptibility of the integrated circuits (IC), whose operation can be disrupted by EM disturbance. Operational amplifier (op-amp) is a common circuit in analog functions, such as signal conditioning stage, bandgap reference or linear voltage regulators, but it can be particularly sensitive to RF disturbance. The parasitic coupled signals can be rectified, leading to EMI-induced offset as described and modelled in numerous scientific books and publications, e.g. [1] [2] [3] [4] [5]. Although the EMI-induced offset in op-amp can be considered as a well-known subject, all the published works considered only continuous wave (CW) disturbance, except [6] where the authors indicated that two-tone interference test can be more appropriate than conventional CW injection to detect all the failures that could be triggered in a real environment.

However, with the growing complexity of EM environments and the increasing concerns about the functional safety of electronic equipment, questions about the EMI-risk assessment of electronic devices in a real environment arises [7]. A particularly important question is the behaviour of electronic devices to multifrequency or multitone disturbance, i.e. composed of several sine waveforms with various amplitude and phase simultaneously injected. Because of the non-linear behaviour of ICs, predicting their response to multifrequency disturbance is not an obvious task. Moreover, testing the susceptibility to multitone EM disturbance can become exponentially long because of the large number of frequency/amplitude/phase combinations, and nothing guarantees that a simplified test procedure, e.g. [8], may have a sufficient coverage level to provide a sufficiently reliable risk assessment.

The purpose of this paper is twofold: first, it aims at clarifying the failure mechanisms that leads to EMI-induced

offset in general-purpose op-amps submitted to a multifrequency disturbance, through experiments and simulations. In this study, only conducted disturbance applied on the non-inverting pin of the op-amp is considered, as it may be connected to long traces and couple EM disturbance. The second objective is to propose a risk assessment method based on CW susceptibility test results to predict the failure threshold of op-amps exposed to multifrequency disturbance. The paper is organized as follows: after a rapid description of the op-amp used as a case study and a brief presentation of its susceptibility to CW disturbance, Section IV analyses the failure mechanisms to multifrequency injection. It highlights the possible links with the CW test results and the limits. Then, a risk assessment method is derived and tested in Section V.

II. PRESENTATION OF THE CASE STUDY

This study relies on a general-purpose op-amp, the reference LMV651 from Texas Instruments. The RF susceptibility of this IC has been studied in [9]. It exhibits the typical failure mechanisms of op-amps to CW disturbance, so the conclusion drawn from this study could be extended to other general-purpose op-amps. Moreover, a simplified behavioural model of this op-amp has been proposed in [9] to simulate the two main mechanisms responsible of the EMI-induced offset: slew-rate (SR) asymmetry and weak distortion (WD) of the input differential pair [1]. This model presents an acceptable accuracy so it is reused in this study to confirm the relevance of experimental results obtained in multifrequency injection.

In this study, the op-amp is mounted in non-inverting configuration. The conducted susceptibility to RF disturbance applied on the non-inverting input pin (V^+) is measured according to the IEC62132-4 Direct Power Injection standard. The experimental set-up is described in Fig. 1. A 50 Ω resistor is mounted at the input to limit the influence of the op-amp input impedance on the conducted susceptibility. An arbitrary waveform generator (AWG) (Anritsu AWG710B) is used to produce both the CW and multifrequency disturbance. The frequency range is restricted between 10 MHz and 1 GHz, due to the bandwidth limitations of the AWG and the RF power amplifier. The EMI-induced DC offset is monitored by a precision voltmeter. The amplitude of the conducted disturbance is given in terms of forward voltage or power and is measured by a power meter through a directional coupler. The presence of harmonics and intermodulation products due to the distortion at V^+ pin is detected by a spectrum analyser which

monitors the reflected voltage. During all the experiments, no distortion of the disturbance applied on the op-amp input was detected, proving that the input impedance of the non-inverting input remains unchanged.

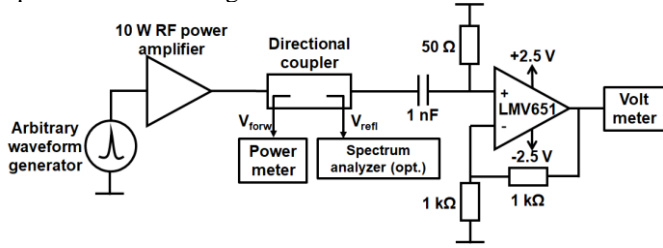


Fig. 1. Experimental set-up

III. SUSCEPTIBILITY IN CW INJECTION

Initially, the susceptibility of the LMV651 to CW disturbance is tested. The AWG is configured to produce a sine waveform. Fig. 2 presents the susceptibility threshold of the op-amp measured for different values of EMI-induced offset (5, 10, 20 and 40 mV). The sign of the offset is also depicted on the graph.

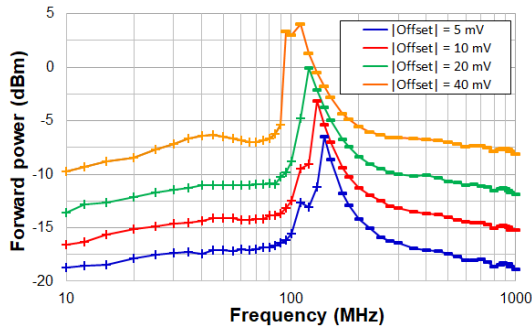


Fig. 2. Susceptibility threshold of the tested op-amp to CW disturbance. '+' means a positive offset and '-' a negative offset.

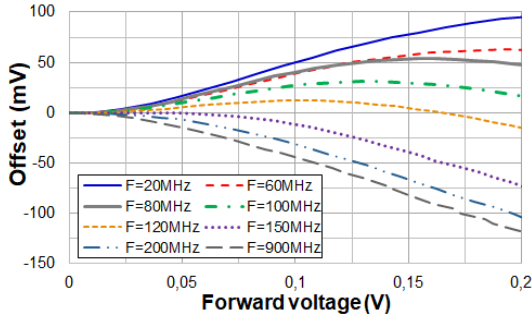


Fig. 3. Evolution of the EMI-induced offset vs. forward voltage at different frequencies.

Up to 100 MHz, the EMI-induced offset is due to the SR rate asymmetry. Due to a larger positive slew-rate, a positive offset is induced. It is interesting to notice that, each time the offset is doubled, the required forward power is increased by 3 to 4 dB. Above 100 MHz, the EMI-induced offset becomes negative and is due to the WD of the differential pair. The gap between the curves is about 3 dB, showing also that the offset does not follow a linear relationship according to the applied voltage. The evolution of the EMI-induced offset at different frequencies is shown in Fig. 3. It shows clearly that the

influence of SR asymmetry tends to be compensated by the WD influence, especially between 80 and 150 MHz.

IV. ANALYSIS OF THE FAILURE MECHANISMS IN MULTIFREQUENCY INJECTION

In this section, the influence of the different failure mechanisms on the EMI-induced offset is analysed in the case of a multifrequency injection. Here, only two-tone injection is considered for clarification purpose.

A. Influence of the Weak-Distortion of the Differential Pair

The EMI-induced offset due to the WD of the differential pair has been extensively used in previous researches, as this mechanism usually dominates above 100 MHz and closed-form expressions of the offset have been derived. This rectification is related to the non-linear relationship between the drain current and the gate-source voltage of the MOSFET forming the input differential pair of the op-amp. Theoretically, for a CW disturbance, the input-related offset at a frequency ω_i depends on the product of the applied differential and common mode voltages (V_{DM} and V_{CM}) applied on the inputs (1) [4], where H_{CM} is related to the structure of the differential pair and parasitic impedance, ϕ the phase of H_{CM} , and θ the phase between V_{DM} and V_{CM} . (1) shows that, ideally, the EMI-induced offset depends on the amplitude A_i of the sine wave applied to the non-inverting input V^+ according to a general quadratic relationship given by (2) and simplified in (3), where the H is a transfer function that depends on the op-amp and its configuration and \bar{X} refers to the average value of X . This trend is confirmed by the experimental result shown in Fig. 4, which presents the evolution of the offset measured on LMV651 output when a 300 MHz sine wave disturbance is applied on V^+ pin. The offset follows clearly a quadratic evolution until the offset reaches -40 mV.

$$V_{off.in} = \frac{-1}{2|V_{gs}-V_T|} V_{DM}(\omega_i) V_{CM}(\omega_i) H_{CM}(\omega_i) \cos(\phi + \theta) \quad (1)$$

$$V_{off}(\omega_i) = H(\omega_i) V^+(\omega_i)^2 = H(\omega_i) A_i^2 \cos(\omega_i t + \phi_i)^2 \quad (2)$$

$$V_{off}(\omega_i) = H(\omega_i) \frac{A_i^2}{2} \quad (3)$$

As suspected in [6], this type of relationship leads to a relatively simple behavior in multifrequency injection. Let consider a multifrequency disturbance composed of N tones with different frequencies ω_i , amplitude A_i and phase ϕ_i . The offset is given by (4), which is actually the sum of the individual contribution of each tone without any influence of their phase (5). The offset is related to the average power of each tone.

$$V_{off} = \overline{\sum_{i=1}^N H(\omega_i) A_i^2 \cos(\omega_i t + \phi_i)^2} = \sum_{i=1}^N H(\omega_i) \frac{A_i^2}{2} \quad (4)$$

$$V_{off} = \sum_{i=1}^N V_{off}(\omega_i) \quad (5)$$

In order to verify this property of the WD on the EMI-induced offset, a two-tone injection test is made with frequencies $F_1 = 300$ MHz and $F_2 = 319$ MHz. The amplitude of the first harmonic V_{forw1} is kept constant, while the amplitude of the second one V_{forw2} is increased. Fig. 5 shows the evolution of the offset according to V_{forw2} , for two different values of V_{forw1} . The theoretical offset is also computed as the sum of the measured offset in CW tests. A good agreement is observed up to an offset of -40 mV, proving that the contributions of both

harmonics sum together. This property is also verified for a larger number of tones (tested up to 40 tones).

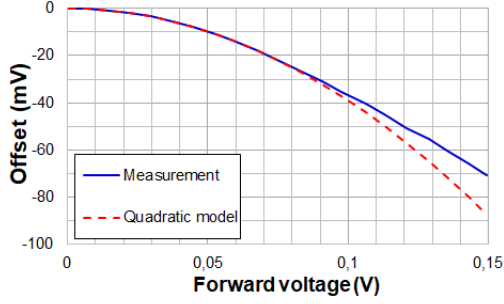


Fig. 4. Measured evolution of the EMI-induced offset when the WD mechanism dominates ($F = 300$ MHz).

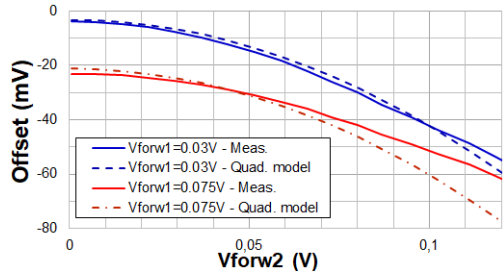


Fig. 5. Evolution of the offset in a two-tone injection test when the WD failure mechanism dominates ($F_1 = 300$ MHz and $F_2 = 319$ MHz)

B. Influence of the Slew-Rate Asymmetry

As reported in numerous research publications, the EMI-induced offset up to several tens of MHz is essentially due to the unavoidable SR asymmetry. Although this phenomenon is well-known, it remains a strong linear distortion which resists to closed-form expressions.

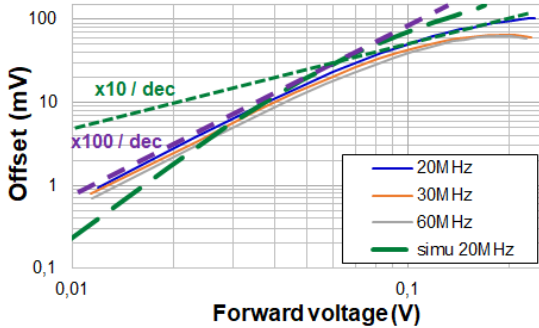


Fig. 6. Measured evolution of the EMI-induced offset when the slew rate asymmetry mechanism dominates.

In CW injection, Fig. 6 shows the evolution of the EMI-induced offset measured according to the disturbance amplitude at three different frequencies where the influence of SR asymmetry dominates. Contrary to the WD, the trend is less clear. As long as the amplitude of the disturbance remains low, the offset tends to increase according to a quadratic evolution. The error with the quadratic model is less than 10 % when the offset does not exceed 20 to 25 mV. Then, the offset increase slows down and tends to a linear evolution for medium amplitude of the disturbance. This type of evolution is confirmed by simulation. For larger amplitude, the positive offset tends to be compensated by the influence of the WD.

A two-tone injection test is made on the op-amp with frequencies ranging from 10 to 100 MHz. Fig. 7 presents the evolution of the measured offset according to V_{forw2} for a constant amplitude V_{forw1} , with $F_1 = 20$ MHz, $F_2 = 29$ MHz and identical phase (changing the phase has actually no effect on the induced offset). The evolution of the offset in CW injection at F_2 is also reported. It appears that the resulting offset is not the sum of the individual contribution of each tone. Moreover, adding a second tone contributes to reduce the offset compared to CW injection, especially if both tones have similar amplitudes. This effect is also observed in simulation, as shown in Fig. 8. The WD has been inhibited in the model to confirm that this effect is intrinsic to the SR asymmetry.

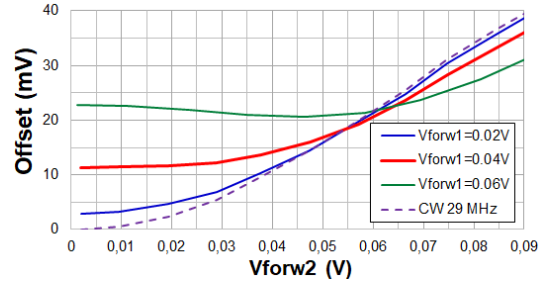


Fig. 7. Evolution of the measured offset in a two-tone injection test when the SR asymmetry failure mechanism dominates ($F_1 = 20$ MHz and $F_2 = 29$ MHz)

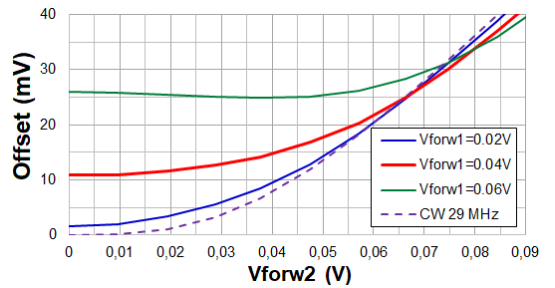


Fig. 8. Evolution of the simulated offset in a two-tone injection test when the SR asymmetry failure mechanism dominates ($F_1 = 20$ MHz and $F_2 = 29$ MHz)

These results reveal the complex non-linear behavior of the SR asymmetry mechanism. In a first approximation, for small offset value, we propose the following model to combine the influence of the different tones on the SR (6). It provides a reasonably good estimation of the offset in the case of a two-tone injection, as shown by Fig. 9, where the error does not exceed 20 % for a maximum offset of 40 mV.

$$V_{off} = \sqrt{\sum_{i=1}^N V_{off}(\omega_i)^2} \quad (6)$$

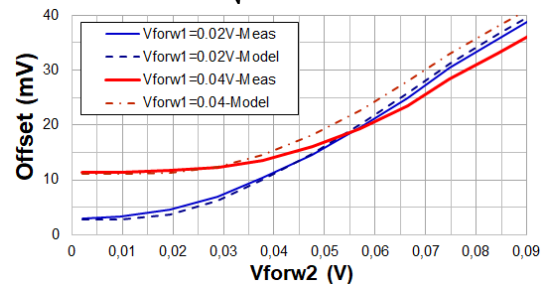


Fig. 9. Comparison between measured and predicted EMI-induced offset with the combination model (6) of the influence of the different tones ($F_1 = 20$ MHz and $F_2 = 29$ MHz)

C. Influence of the Signal Asymmetry

An interesting and unexpected effect is observed when several tones with frequencies multiple of the first one are injected. For example, let consider a two-tone injection, where both tones have the same amplitude (P_{forw} of each harmonic is set to -12 dBm) and are in-phase. The frequency F_1 of the first tone is set to 20 MHz while the frequency F_2 of the other tone is swept between 8 and 105 MHz. The polarity of the injected signal can be reversed (i.e. the sign of each tone is inverted in the AWG) so that the test is repeated for both signal polarity, called positive and negative. The measured offset is plotted in Fig. 10. As confirmed by previous results, the offset stabilizes around a nearly constant value above 15 MHz, except at 20 MHz where both tones have the same frequency. The polarity of the signal has no influence, except at some particular frequency combinations where there is an even factor between tone frequencies (e.g. at 10, 30, 40, 60, 80 and 100 MHz). The offset can be seriously increased or decreased, and is also dependent on the phase of the tones. For these combinations, the waveform is pulse-like and the distribution of the amplitude becomes asymmetrical. This asymmetry tends to decrease when the separation between both tones increases.

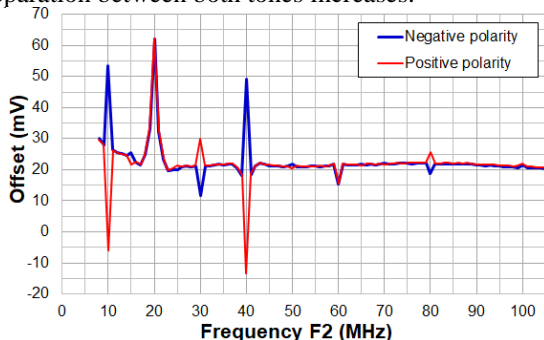


Fig. 10. Evolution of the offset in a two-tone injection test with identical amplitude ($F_1 = 20$ MHz)

Here, another mechanism offset, still related to the SR limitation of the op-amp, is activated. The rectification is not only due to SR asymmetry, but also to the asymmetry of the signal. This effect has not been detected in previous studies about EMI-induced offset in op-amps since only CW signals were considered. For example, with $F_1 = 20$ MHz, $F_2 = 40$ MHz and a positive polarity, the applied signal is a positive pulse, which is rectified due to the SR limitation. A reduction of the average value of the signal is obtained which counterbalances the offset due to the SR asymmetry. The same effect is also visible when the influence of WD dominates.

Fig. 11 presents the evolution of the offset in two-tone injection with frequencies related by a factor 2, when the SR asymmetry mechanism dominates (top figure) and the WD dominates (bottom figure). The test is repeated for both polarities and shows large differences, which are not observed when one frequency is slightly changed. It is interesting to notice that the average value between the offsets measured in positive and negative polarities tend to the offset only due to SR asymmetry or WD. These results prove that the offset due to these known mechanisms add to the offset due to the signal asymmetry, which can be considered as an independent source

of offset. In low frequency, the offset due to the signal asymmetry evolves at the same rate than the offset due to SR asymmetry as long as the offset remains small. Then, it increases quasi-linearly, as confirmed by simulation. In high frequency, when the WD mechanism dominates, the contribution of the signal asymmetry remains negligible for small offset values and, then, tends to increase rapidly. This effect is also confirmed by simulation.

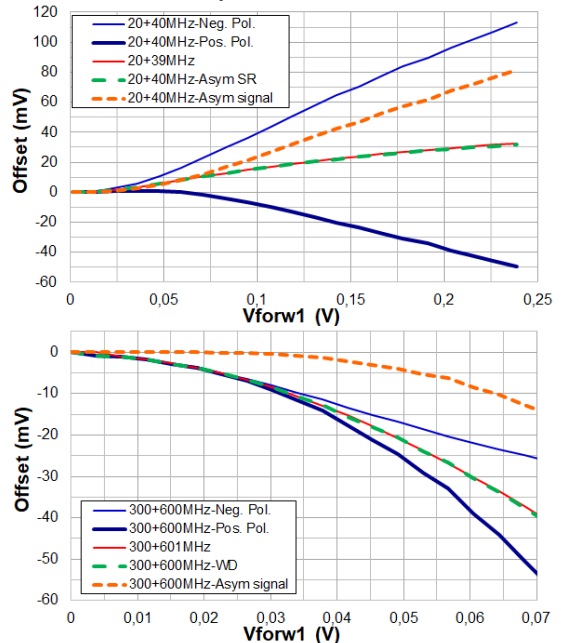


Fig. 11. Impact of the signal asymmetry: when the SR asymmetry dominates (top) and the weak distortion dominates (bottom)

V. ASSESSMENT OF THE RISK OF FAILURE DUE TO EMI-INDUCED OFFSET IN MULTIFREQUENCY INJECTION

A. Description of the Assessment Method

The analysis done in the previous section proves that the exact computation of the EMI-induced offset in multifrequency injection is not an obvious task because of the non-linear behaviour of op-amp and the simultaneous existence of several failure mechanisms. The failure assessment in multifrequency injection can become a complex and tedious task if the susceptibility of the op-amp has to be tested with a large number of combinations of frequency, amplitude and phase. However, different observations can be used to determine the risk of EMI-induced offset failure from the CW susceptibility test results, especially for small to medium offset values (less than several tens of mV) which correspond to usual failure criterion level in typical analog functions. Here, we neglect the case of multifrequency injection with frequencies related by an even factor, as it is a particular case. This specific case will deserve additional work.

Firstly, let consider the offset due to WD mechanism. (5) shows that the offset in multifrequency injection is only the sum of the offset produced individually by each tone, which depends on the average power of the tone. Although the failure mechanism is intrinsically non-linear, an equivalent of the superposition principle applies here for the failure, called

disturbance superposition principle as introduced in [10]. It allows a simple correlation between CW and multifrequency susceptibility levels when the failure results from the linear superposition of the contribution of each injected harmonic. If the electronic device is submitted to multifrequency disturbances composed of M harmonics with frequencies f_k and amplitudes E_k , $k \in [1; M]$, this principle is met if (7) is verified. S_k is the susceptibility threshold of the DUT to CW disturbance measured at a frequency f_k and I_{tot} is the interference coefficient. The impact of each harmonic is weighted by the CW susceptibility threshold in order to account for the susceptibility of the DUT at frequency f_k . When the sum of the weighted harmonics exceeds 1, the failure arises.

$$I_{tot} = \sum_{k=1}^M \frac{E_k}{S_k} = 1 \quad (7)$$

When the WD dominates, (4) shows that the EMI-induced offset results of the sum of the contributions of the average power of each injected harmonic. Thus (7) is verified with the term E_k and S_k expressed in term of average power P_{Ek} and P_{Sk} (8).

$$I_{totWD} = \sum_{k=1}^M \frac{P_{Ek}}{P_{Sk}} = 1 \quad (8)$$

Secondly, for the offset due to SR asymmetry, results of IV.B show that, for an offset that does not exceed several tens of mV, the offset increases with the applied voltage according to a quadratic relationship in CW injection, i.e. it depends on the average power of the applied CW disturbance. Moreover, the offset in multifrequency injection can be approximated as the square root of the sum of square of the offset due to each applied tone (6). Therefore, another form of disturbance superposition principle applies here and the interference coefficient I_{totSR} can be defined by (9) and simplified into (10), where $offset_{meas}$ is the offset measured in the tested multifrequency injection scenario and $offset_{max}$ is the maximum allowed offset defined for the susceptibility test.

$$I_{totSR}^2 = \frac{offset_{meas}^2}{offset_{max}^2} = \sum_{k=1}^M \left(\frac{P_{Ek}}{P_{Sk}} \right)^2 \quad (9)$$

$$I_{totSR} = \sqrt{\sum_{k=1}^M \left(\frac{P_{Ek}}{P_{Sk}} \right)^2} \quad (10)$$

From the CW susceptibility test results obtained for a given definition of the maximum offset, (8) and (10) offers a simple method to determine whether a combination of M tones may lead to a failure ($offset > offset_{max}$). This situation may happen if I_{tot} exceeds 1. These formulas may be used only if all the tones activate either the WD mechanism (8) or the SR asymmetry

(10). In the case where M_1 tones activate the WD mechanism and M_2 tones the SR asymmetry, the offset due to both mechanisms adds together and (11) can be used to determine the interference coefficient, where $sign_{WD}$ and $sign_{SR}$ give the offset due to WD and SR respectively.

$$I_{tot} = sign_{WD} \sum_{k=1}^{M_1} \frac{P_{Ek}}{P_{Sk}} + sign_{SR} \sqrt{\sum_{k=1}^{M_2} \left(\frac{P_{Ek}}{P_{Sk}} \right)^2} \quad (11)$$

B. Validation

In order to validate the failure assessment method, three and four tones test are made on the op-amp. Two limits for the maximum offset are considered: ± 10 and ± 20 mV. The CW susceptibility thresholds for these failure criteria are known and given in Fig. 2. For each test, a combination of three or four frequencies (without even factor between frequencies) is selected with different amplitudes. Phases are identical but tests show that the phase has no significant influence. The amplitude of the third or fourth harmonic is increased while the others keep a constant value. For each amplitude, the interference coefficient is computed and the offset is monitored.

Figs 12 and 13 compare the computed interference coefficient and the measured offset, either for frequencies ranging between 200 and 1000 MHz (WD dominates) and between 10 and 100 MHz (SR asymmetry dominates). The failure limit is reached when the absolute value of the offset exceeds 10 or 20 mV, and when the interference coefficient exceeds 1. The results show that there is a good agreement between the evolution of the interference coefficient and the offset, especially closed to the failure threshold. For injection made between 200 and 1000 MHz, the difference between the measured susceptibility threshold and the limit given by $I_{tot} = 1$ does not exceed 5 %, i.e. an error less than 0.4 dB. For injection made between 10 and 100 MHz, this difference does not exceed 6 %, i.e. an error less than 0.5 dB. The same test is repeated for frequencies ranging between 10 and 1000 MHz, thus activating both failure mechanisms. A good agreement is also observed between the evolution of I_{tot} and the measured offset (Fig. 14). The difference between the measured susceptibility threshold and the limit given by $I_{tot} = 1$ does not exceed 6 %, i.e. an error less than 0.5 dB. These results prove that, for small maximum offset value, the evaluation of the interference coefficient given by (8), (9) or (10) provides a simple method to determine if a combination of several tones reaches the susceptibility threshold of an op-amp.

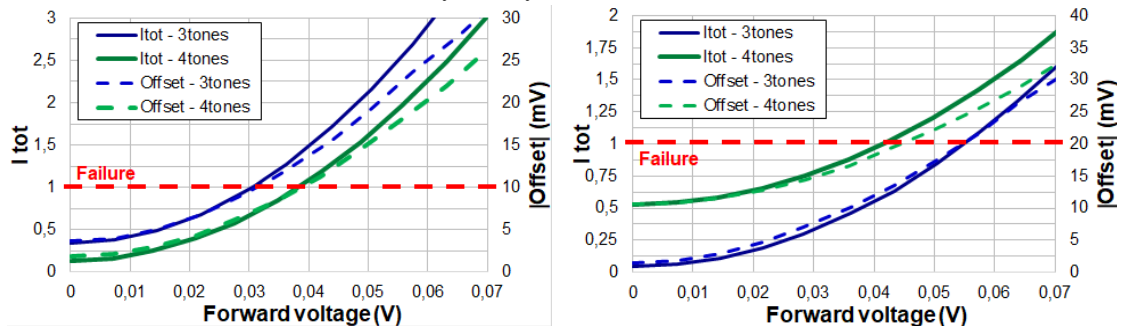


Fig. 12. Risk assessment when the WD dominates for a maximum EMI-induced offset of 10 mV (left) and 20 mV (right). $F_1 = 271$ MHz, $F_2 = 336$ MHz, $F_3 = 802$ MHz, $F_4 = 559$ MHz.

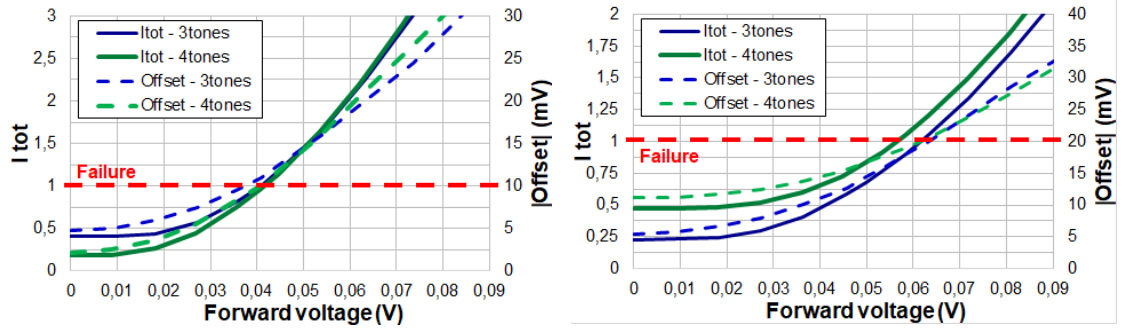


Fig. 13. Risk assessment when the SR asymmetry dominates for a maximum EMI-induced offset of 10 mV (left) and 20 mV (right). $F_1 = 23$ MHz, $F_2 = 49$ MHz, $F_3 = 81$ MHz, $F_4 = 57$ MHz

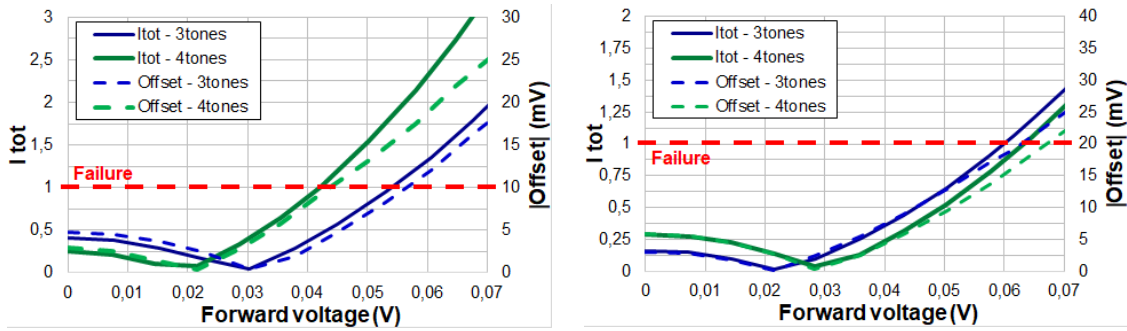


Fig. 14. Risk assessment with both failure mechanisms, for a maximum EMI-induced offset of 10 mV (left) and 20 mV (right). $F_1 = 23$ MHz, $F_2 = 49$ MHz, $F_3 = 336$ MHz, $F_4 = 802$ MHz

VI. CONCLUSION

This paper has presented an in-depth analysis of the failure mechanisms responsible of EMI-induced offset in an op-amp submitted to multifrequency injection. In addition to the well-documented WD and SR asymmetry mechanisms, the paper has revealed the influence of the signal asymmetry as another source of offset in multifrequency injection. In spite of the non-linear behaviour of op-amps, the paper has determined general trends in the evolution of the offset according to the disturbance amplitude and in the combination of the different injected tones, for small offset values. From these results, a method has been proposed to determine if an op-amp exposed to a given combination of tones may reach the failure limit. As the approach relies only on CW susceptibility test results, it provides a simple method to estimate the risk of failure in multifrequency injection.

The obtained results have been extracted from experiments done on a general-purpose op-amp and confirmed by simulations on a general behavioural model. The results should be certainly extrapolated to other op-amps, which will be confirmed in future studies. The proposed failure assessment method does not consider the effect of the signal asymmetry on the EMI-induced offset. Further works will be necessary to include this effect.

REFERENCES

- [1] J. M. Redouté, M. Steyaert, *EMC of Analog Integrated Circuits*, Springer, 2010.
- [2] G. Masetti, S. Graffi, D. Golzio, ZS. M. Kovacs, "Failures induced on Analog Integrated Circuits by conveyed Electromagnetic Interferences: a Review", *Microelec. Rel.*, vol. 36, no 7/8, pp. 955-972, 1996.

- [3] J. G. Tront, J. J. Whalen, C. E. Larson, J. M. Roe, "Computer-Aided Analysis of RFI Effects in Operational Amplifiers", *IEEE Trans. on EMC*, vol. 21, no 4, Nov. 1979.
- [4] F. Fiori, "A New Nonlinear Model of EMI-Induced Distortion Phenomena in Feedback CMOS Operational Amplifiers", *IEEE Trans on EMC*, vol. 44, no 4, pp. 495-502, Nov. 2002.
- [5] A. Richelli, "EMI Susceptibility Issue in Analog Front-End for Sensor Applications - Review article", *Journal of Sensors*, 2016.
- [6] F. Fiori, M. Brignone Aimonetto, "Measurement of the Susceptibility to EMI of ICs with Two-Tone Interference", in *Proc. of APEMC 2018*, pp. 292 - 296, Singapore, May 2018.
- [7] D. Pissoort, K. Armstrong, "Why is the IEEE developing a standard on managing risks due to EM disturbances?", in *Proc. of IEEE Int. Symp. on EMC*, pp. 78-83, Ottawa, Canada, Sep. 2016.
- [8] W. Grommes, K. Armstrong, "Developing Immunity Testing to Cover Intermodulation", in *Proc. of IEEE Int. Symp. on EMC*, pp. 999-1004, Long Beach, CA, USA, Aug. 2011.
- [9] A. Boyer, E. Sicard, "A Case Study to apprehend RF Susceptibility of Operational Amplifiers", *12th Int. Workshop on the EMC of Integrated Circuits (EMC Compo 2019)*, Hangzhou, China, Oct. 21-23 2019.
- [10] A. Boyer, F. Caignet, "A Pre-Scan Method to Accelerate Near-Field Scan Immunity Tests", *IEEE Lett. on EMC Practice and Applications*, Early Access, Feb. 2024, 10.1109/LEMCPA.2024.3363113.